EXPERIMENTAL STUDY OF ACOUSTIC STREAMING INDUCED BY A SHARP EDGE AT DIFFERENT FREQUENCIES AND VIBRATING AMPLITUDES

Hui CHEN[1], Geyu ZHONG[2], Chuanyu ZHANG[3*], Dan LIU[4], Xueyong WEI[3], Yingwen LIU[1†]

[1]Key Laboratory of Thermo-Fluid Science and Engineering of MOE, School of Energy and Power Engineering, Xi'an Jiaotong University, Xi'an, 710049, Shaanxi, China

[2]Science and Technology Research Institute, China Three Gorges Corporation, Beijing 100038, China

[3]State Key Laboratory for Manufacturing Systems Engineering, Xi'an Jiaotong University, Xi'an, 710049, Shaanxi, China

[4]State Key Laboratory of Cancer Biology and National Clinical Research Center for Digestive Diseases, Xijing Hospital of Digestive Diseases, Fourth Military Medical University, Xi'an, China

Corresponding authors; [*]E-mail: chuanyu.zhang@xjtu.edu.cn; [†]E-mail: ywliu@xjtu.edu.cn

Acoustic streaming is the time-averaged flow induced by acoustic waves inside the fluid medium. Much attention has been paid to the streaming flow at the microscale, with the rapid development of microfluidics and significant demand for the microscale manipulation of fluid or particles. Recently, the streaming flow at the audible or lower frequency (10 Hz ~ 10 kHz) has been found to be closely associated with local structures, like a sharp edge in the microchannel. By its strong magnitude and low cost, this kind of streaming flow has been applied in various fields. However, the mechanisms behind this non-classical Rayleigh streaming are still not very clear, though its high sensitivity to the thickness of the acoustic boundary layer and unstable streaming pattern under high forcing amplitude have been demonstrated. In this study, experimental work has been conducted, with the help of the Particle Imaginary Velocimetry (PIV) platform, to reveal the influence of frequency and vibrating amplitude on the streaming flow field around a sharp edge with 90◦, and its characterized spatial dimension. The scaling law concerning the vibration amplitude and streaming velocity has been come up with, and the parameter frequency is also included. The expression $f^{-1/6}v_a^2 \sim v_{sy,max}$ *demonstrates a good prediction in terms of the streaming magnitude, in comparison with experimental results.*

Keywords*: Acoustic streaming; Sharp edge; Parametric study*

1. Introduction

Acoustic streaming (AS) is a time-averaged steady flow generated by an acoustic field in a fluid. The special phenomenon originated from observation by Faraday[1] and Boluriaan[2]. They found the light particles on vibrating plates move from node to antinode first, and then come back to node. From the perspective of the mechanism of the streaming phenomenon, the formation of this kind of time-averaged flow originates from the energy dissipation of the alternating flow process within the

fluid[3–5]. When sound waves propagate through working fluids, both the velocity and pressure of the fluid undergo alternating oscillations. Without viscous dissipation, the acoustic streaming is generated along the direction of propagation, and this flow is denoted as Eckart streaming[3, 6]. Its induced frequency is at the MHz level. Being different from the Eckart type, the Rayleigh streaming is closely associated with the viscous Stokes boundary layer near the wall[7]. It is usually caused in low viscous liquids and relatively low frequency (<1 MHz) viscous dissipation. The thickness of this dissipation region can be calculated by the Stokes boundary layer $\delta = \sqrt{2\vartheta/\omega}$, where υ and ω represent kinematic viscosity and angular frequency of alternating flow respectively.

In recent decades, low-frequency vibrations have been a research hotspot in household devices, transportation vehicles, industrial machines, and human motions. Particularly in recent years, AS attracts increasing attention in heat transfer fields. This low-frequency vibration-induced streaming flow vortex is a means of enhancing heat and mass transfer[8, 9]. Furthermore, the longer wavelength of low-frequency sound waves makes it possible to expand the study of streaming flow from the microscale to the millimeter scale, providing a new perspective for the study of alternating flow phenomena.

Huang et al.[10–12] observed a streaming flow induced near the sharp structures and applied it to the enhancement of mass transfer in 2013. Afterward, Ovchinnikov et al.[13] provided theoretical and numerical explanations for this phenomenon. Costalonga et al.[14] vibrated the beams with different geometric ends inside the fluid. With oscillation frequencies from 50 Hz to 200 Hz, they have demonstrated the effect of the frequency and amplitude of the forcing vibration on the streaming vortices. In recent years, Zhang et al.[7, 14, 15] have conducted experimental and theoretical research on the streaming flow characteristics of sharp corners. This streaming phenomenon at low frequency, appearing in more and more scenarios[16, 17], is found to exhibit several features.

The streaming flow at audible or lower frequency has closely associated with specific local structures. The critical condition to induce streaming near sharp corners relies on the ratio of the characteristic diameter of curvature rc of the corners' tip to the thickness of the acoustic viscous boundary layer δ [18]. So both local geometric size and acoustic frequency will influence the appearance of streaming flow. This requires highly accurate machining of local structures, which now are generally achieved through lithography at the microscale. Therefore, lower exciting frequency, corresponding to a thicker acoustic boundary layer, can reduce the difficulty of sharp corner machining. It can be easily realized by conventional machining, laser cutting, or 3D printing. In addition, compared to the Rayleigh streaming excited under ultrasonic frequency conditions in the past[6], this low-frequency streaming flow, in the range of 10 Hz to 10 kHz[19, 20], allows a wider selectivity for vibration sources.

At present, the mechanisms and critical physical scaling effects are still not very clear though much attention has been paid to the low-frequency time-averaged flow phenomenon. Previous research mainly focused on the maximum streaming flow velocity $v_{sy,\max}$ along the radial direction of the channel, and obtained the quadratic relationship $v_{sy,\max} \sim v_a^2$ between the maximum streaming flow and the amplitude of the alternating velocity v_a. Ovchinnikov et al.[13] came up with a theoretical model for a quantitative description of streaming velocity for absolute sharp corners (curvature radius of sharp corners r_c =0), and found that the streaming velocity v_s and vibration velocity v_a at sharp corners exhibit a relationship $v_{sy} \sim v_a^2 h/\upsilon$. If substituting the acoustic amplitude $A=v_a/(2\pi f)$, $v_s \sim A^2 f^2 h$ can be obtained, including the frequency and viscosity. In addition, by introducing the mechanical vibrator

to excite the streaming flow, a much larger vibration amplitude can potentially be adopted, where this type of vibration drive can be achieved through ordinary vibrators or subwoofers. And some characteristics of the flow vibration will change compared to low- amplitude forms ($A<r_c$, $A<\delta$)[21]. Especially, previous studies[22, 23] have found that the transient state of alternating vibrating of fluids may change with the increase of driving amplitude, forming complex vortex shedding modes that are relatively independent or mutually influencing at specific positions. The formation of these complex vortices is likely to actively affect the streaming jet along the transverse channel from the tip of the sharp edge structure.

Based on the above analysis, concerning the sharp edge streaming, the relation of the maximum velocity of the streaming flow to the frequency and vibrating amplitude is still not very clear, especially with respect to the practically machined curvature of the edge with an angle of 90°. To find out some features and the influence of parameters of different operating conditions on the time-averaged flow phenomenon, with the help of Particle Imagnery Velocimetry (PIV), this paper mainly carries out an experimental study of streaming flow induced by low-frequency excitement inside the microchannel in the vicinity of a sharp edge. The effect of vibrating frequency and forcing amplitude on the streaming flow is discussed by characterizing the streaming velocity and the spatial dimension. A fitting expression including the parameter of frequency is correlated to provide a further understanding of the acoustofluidics at an audible or lower frequency.

2. Experimental setup and testing method

2.1. Experimental setup

As shown in Figure 1, the testing system includes the signal system (which includes the signal generator, amplifier, oscilloscope, and piezoelectric transducer), optical testing system (includes high-power blue light, microscope, high-speed camera, and PC), and the liquid path (which includes two syringe pumps and the glass-PDMS chip with sharp edge included).

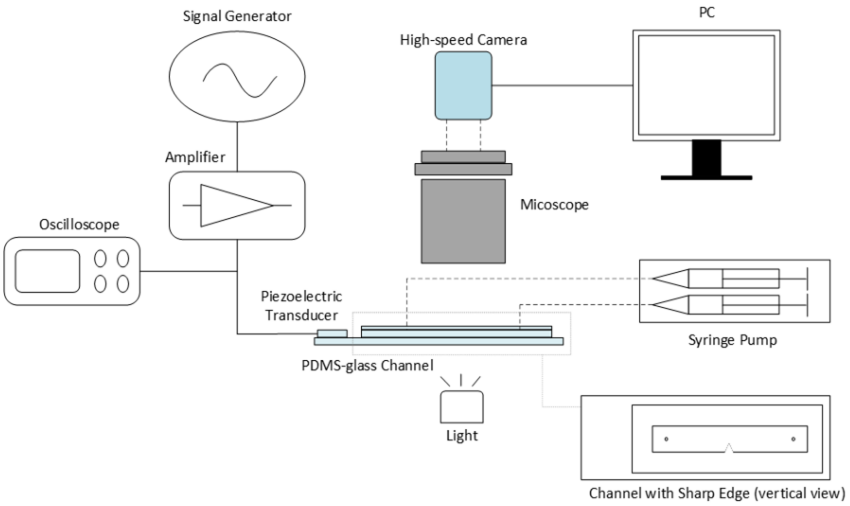

Figure 1. The brief diagram of the experimental setup

The vibration is induced by the piezoelectric transducer attached to the surface of the glass chip. Therefore, the power is transferred from the amplifier to the oscillation of liquid in the PDMS channel. Basically, the displacement of the particles has a linear relationship with the voltage of the amplifier,

especially at low voltage. For the visualization of the particles, we employed the seeded particles are fluorescent (excitation wavelength 480 nm, light emission wavelength 515 nm), and found that under some conditions of lighting, and due to the limited sensitivity of the camera, the diffused light could offer better contrast than the fluorescence-emitted light. Therefore, the motion of the liquid in the microchannel can be observed by the microscope.

2.2. Fabrication of PDMS chip

The microchannel is built around a Y-shaped Polydimethylsiloxane (PDMS) microchan- nel devised by standard photolithography techniques: starting from a SU8 resist-made mould of thickness 50 mm made on a silicon wafer, a mixture of PDMS (Sylgard 184) with 10% in the mass of curing agent is poured on the SU8 mould and forms a 2.5-mm-thick layer on top of the wafer. After baking at 338 K for 4 hours, the PDMS mixture is then sealed and attached to a glass coverslip after a 1 mn O_2 plasma treatment of both faces. A PDMS microchannel of depth p =50 mm is then obtained. The width w is equal to 500 mm. Sharp edges with different angles could be fabricated from various moulds. The degree with 90° is fabricated in this study.

2.3. Visualisation of acoustic streaming

The fluorescent particles are spread homogeneously in the liquid with a diameter of 1.0 μm or 4.9 μm. As shown in Figure 2. In this study, an acceptable contrast and high-quality image can be obtained by diffusion under blue light. The depth of field of the microscope lens is about 10 μm. The channel depth is 50 μm. Through the adjustment of focus, clear high-fidelity images can be captured. The height of the channel is 500 μm. The pixel scale is about 0.588 pixels/μ, which can be employed to capture the granular motion of the fluid clearly.

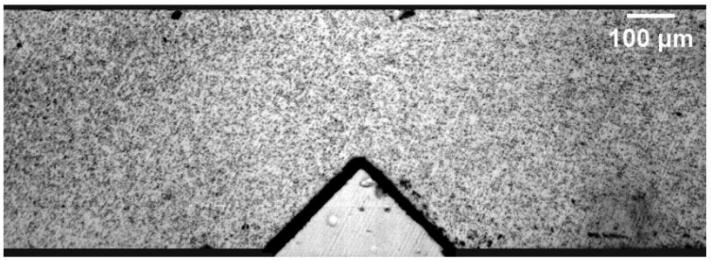

Figure 2. The visualization of PDMS chip filled with the fluorescent-particles

Before measuring the displacement amplitude of the fluid in the channel, the vibration of the glass is analyzed. In general, the vibration in the glass and fluid in the channel will be influenced significantly by the adhesion mode between the piezoelectric transducer and the glass, the location of the sensor, and the structures of the channel. At present, there is no available research on fluid vibration on micro-scale structures within the audible frequency range. However, it's found that there is no relative displacement between the sharp edge structure and the glass, according to the existing experimental results. In order to understand the motion response between the glass substrate and fluid under vibration conditions, the laser Doppler vibrometer was used to measure the vibration of the glass substrate. The Polytec OFV-5000 Modular Vibrometer is used to measure the displacement amplitude of the glass driven by the piezoelectric sensor on the optical platform. It was found that the displacement amplitude of the glass is approaching 0.005 ~ 0.35 μm when the peak-to-peak voltage

V_{pp} was 60 V under the driving frequency of 3 kHz, which is much smaller than the measured displacement amplitude of oscillating fluid.

The coupling relationship between piezoelectric materials and glass sheets is very complex, as proposed by Dual et al.[24]. Although the research shows that the glass chip is excited by the piezoelectric transducer attached to it to generate vibration, the mechanism of the vibration in the microchannel is still unclear. According to previous experimental measurements, the different sticking positions of piezoelectric materials on the glass chip will significantly affect the vibration amplitude of the fluid in the channel.

2.4. Methods for testing of velocity amplitude and streaming velocity

In order to quantify the movement of particles in an acoustic cycle, the particle displacement image of a single acoustic cycle after the time-averaged streaming flow is stabilized is dynamically photographed. The frame rate of the high-speed camera is set to 25 kHz, and the exposure time is set to 25 μs. Because the exposure time is far less than the vibration cycle, it can meet the shooting requirements multiple times in a cycle, and the particle image is clearly visible. Then, the captured particle image is post-processed, and the amplitude of alternating flow displacement in a single motion cycle is directly measured from the captured image. For the suspended particles far from the sharp corner in the flow passage, the displacement amplitude A is the same, as shown in Eq.1.

$$2A = \int_{\frac{n}{f}}^{\frac{n}{f}+\frac{1}{2f}} v_a \sin(2\pi f)\mathrm{d}t \tag{1}$$

where *A*, *f*, *t*, and *n* represent the fluid displacement amplitude, vibration frequency, time, and the n-th acoustic cycle, respectively.

The vibrating amplitude of fluid in the microchannel under a certain vibration condition can be obtained using Eq.1. Figure 3 shows the measured velocity amplitude response of vibrating fluid driven by different voltages of the piezoelectric transducer. The overall velocity amplitude increases with the voltage and frequency, showing a linear response, as shown in Eq.2, under high frequency and low voltage.

$$v_a = A\omega \tag{2}$$

To obtain the streaming velocity v_s, we select a sequence of images within an acoustic cycle as the time interval to calculate v_s, as shown in Figure 4. PIVlab is employed (https://pivlab.blogspot.com/) to quantify the feature of the streaming flow by detecting the displacement of particles after a full acoustic cycle. At the same time, the streamlining and the vortex of particles can be clearly extracted.

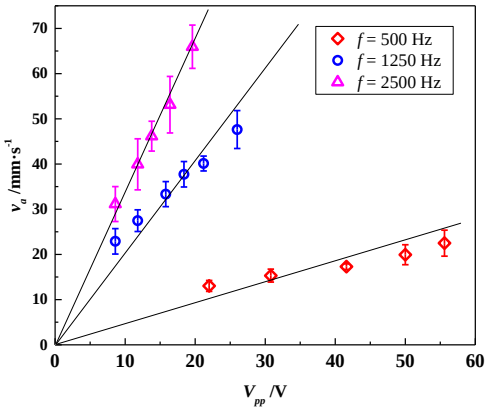

Figure 3. Relationship between peak-to-peak voltage and vibrating amplitude

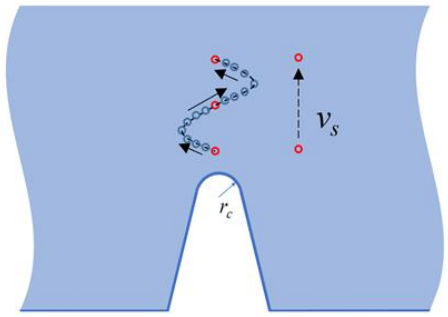

Figure 4. The schematic diagram for testing streaming velocity

3. Results and discussion

3.1. Streaming velocity at different vibrating velocities

The testing conditions in this study are shown in Table I. Within the frequency range of 200 Hz ~ 2500 Hz and the vibrating amplitude of 7.0 mm/s ~ 66 mm/s, the maximum streaming velocity along the normal direction of the sharp edge is extracted. The measured tip angle is 90◦ and the curvature diameter of that is 18.5 ± 3.6 μm.

Table 1. Working conditions of sharp-edge acoustic streaming

Frequency/Hz	Vibrating velocity/mm·s −1	The thickness of Boundary Layer/μm
200	7 ~ 25	39.9
500	13 ~ 23	25.2
800	10 ~ 27	20
1250	23 ~ 48	16
2500	31 ~ 66	11.3

Figure 5 shows the PIV vector diagram of the sharp angle time averaged streaming flow induced by the alternating flow when the amplitude of the alternating speed is 40 mm/s~65 mm/s at 2.5 kHz. In order to better carry out the streaming flow intensity observation, the same observation scale is used for all working conditions. The results show that the greater the amplitude of the alternating velocity, the stronger the time-averaged streaming flow induced. In terms of quantity, the maximum velocity of the time-averaged streaming flow generated under each velocity amplitude is 0.60 mm/s, 0.95 mm/s, 1.34 mm/s, and 2.1 mm/s. The acoustic flow velocity is generated from the top of the sharp corner and reaches the maximum near the sharp corner. For the area far away from the sharp corner, the time average effect of the alternating flow gradually weakens and approaches zero. In the process of streaming flow from the position close to the sharp corner wall to gradually away from it, the size of the time-averaged streaming flow first increases, and then gradually decreases, and the position where the maximum time-averaged streaming flow velocity occurs is similar. Quantitatively,

the amplitude of fluid displacement is relatively small at a large driving frequency, which ranges around 2.9 μm ~ 6.1 μm and is smaller than the curvature diameter of the sharp edge r_c.

From Figure 6, the velocity profiles of the streaming flow along the normal direction of the sharp edge can be observed with the peak-to-peak voltages of 11.8 V and frequencies of 800 Hz, 1250 Hz, and 2500 Hz respectively. From the distribution features, the streaming flow gradually increases from the top of the sharp corner and approaches to its maximum value near the viscous boundary layer with those of 0.1 mm/s, 0.4 mm/s, and 0.6 mm/s, respectively. Besides, the error of the velocity measurement also shows a trend of increase-to-decrease, which means a high error in the middle and low on both sides. At the same time, with the increase in frequency, the thickness of the viscous boundary layer decreases. At the position far away from the sharp tip and close to the wall, the streaming velocity is approaching zero due to the blocking of the wall, which restricts the streaming jet. As shown in Figure 6, the distribution of streaming velocity at f=2.5 kHz shows an accelerated attenuation of streaming velocity after y=0.22 mm. At the same time, the suppression of streaming vortices caused by the wall appears. This wall restriction influences the spatial shape of the vortex, which will be discussed in the following part.

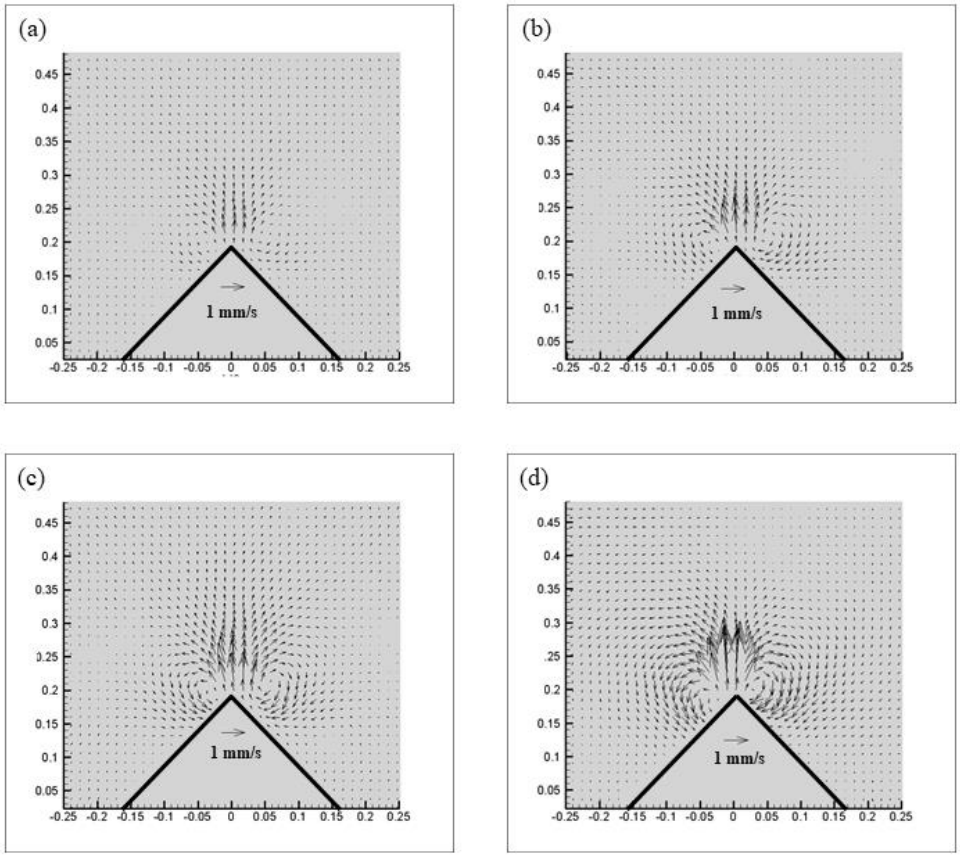

Figure 5. Vectors of sharp edge streaming velocity at different forcing velocities with f =2.5 kHz, (a) v_a = 40 mm/s, (b) v_a = 46 mm/s, (c) v_a = 53 mm/s, and (d) v_a = 65 mm/s

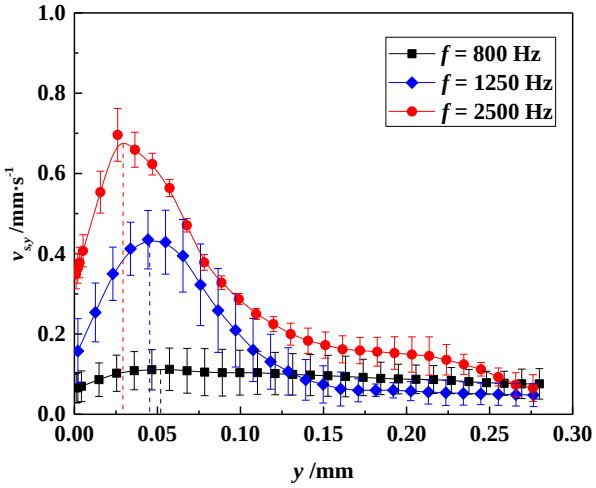

Figure 6. Distribution of streaming velocity along the normal direction of the sharp edge, δ_{2500Hz}= 11.3μm, δ_{1250Hz}= 16μm, δ_{800Hz}= 20μm

Quantitatively, under different vibrating frequencies of 800 Hz, 1250 Hz, and 2500 Hz, the distances of corresponding maximum streaming velocities $v_{sy,\,max}$ from the sharp edge are 51.0 μm, 44.9 μm, and 28.9 μm. Compared with the thickness of the boundary layer obtained by theoretical calculation as shown in Table 1, the position to the maximum streaming velocity from the top of the sharp tip is about 2.5 ~ 2.8 times the thickness of the boundary layer, as shown in Figure 7. Limited by the lighting conditions, the light beam is difficult to set perpendicular to the glass. Therefore, the shadow area (as shown in Figure 2) is introduced near the wall boundary due to optical projection during image shooting. It will bring a deviation of 20 μm at the position measurement of the streaming velocity profile. However, by repetitive experiments, it can be found that the maximum streaming velocity occurs near the thickness of the boundary layer.

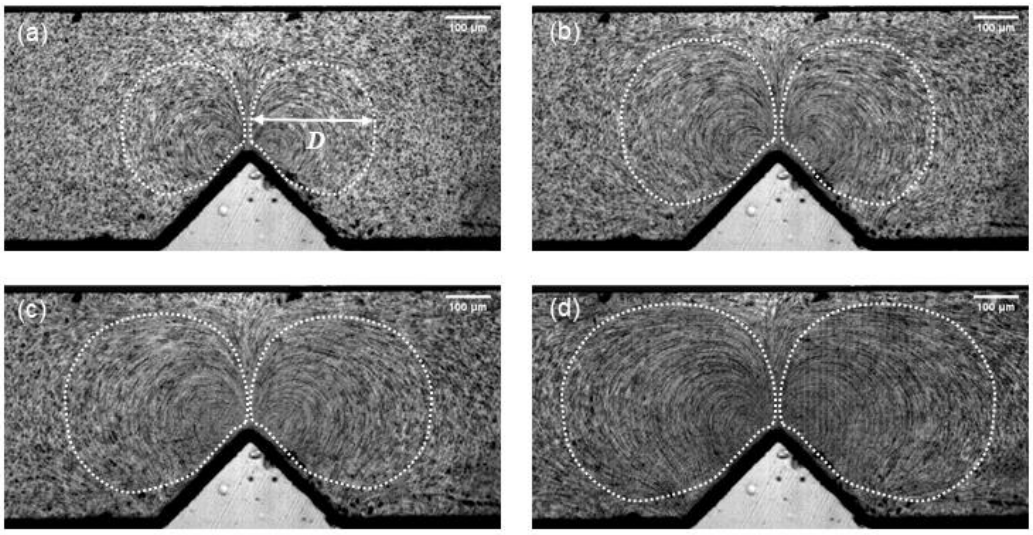

Figure 7. Vortex diameter D of streaming vortex under different forcing amplitudes, f= 1250 Hz, (a) v_a= 23 mm/s, (b) v_a= 33 mm/s, (c) v_a= 40 mm/s, and (d) v_a= 48 mm/s

3.2. Spatial characteristics of streaming vortice pair

Figure 7 shows the particle migration with the acoustic streaming at 1.25 kHz and different forcing velocities v_a of 23 mm/s, 33 mm/s, 40 mm/s, and 48 mm/s, respectively. Therefore, the

characteristics of streaming vortices can be studied after the streaming flow reaches its stable state. It can be clearly observed that the maximum vorticity is in the vicinity of the sharp edge, where the dissipation occurs intensively. Besides, with the increase of forcing velocity, the influenced domain of the streaming vortex becomes larger. At the same time, the shapes of vortices are also affected by the increase of forcing amplitude, say the vortex will be squeezed when the acoustic flow area is large as shown in Figure 7-d.

In order to quantify the spatial characteristics of the acoustic flow vortex, the streamlined diagram of the sharp corner acoustic flow is analyzed. As shown in Figure 7-a, the vortex diameter D of the vortex in the transverse direction of the flow channel is defined. After measuring the scale of the mentioned domains at different frequencies and forcing velocities, the spatial characteristics are presented in Figure 8(a). We can find that the vortex diameter of streaming vortices increases nearly linearly with the vibrating velocity. A linear fitting function, Eq.3, is defined to conduct the linear fitting.

$$D = av_a \tag{3}$$

where D, v_a, a represent the vortex diameter of streaming vortex/μm, the vibrating velocity/mm·s^{-1}, and the linear fitting coefficient/10^{-3} s.

What should be noticed is that the fitted coefficients are 30.8, 17.9, 16.1, and 9.7 which are obtained at different frequencies of 200 Hz, 500 Hz, 800 Hz, and 1250 Hz, respectively, with R^2 >0.98. To further quantify the relationship between D and v_a at different frequencies and vibrating velocities, the relationship of fitted coefficient and frequency $a \sim f^{(-0.6)} \sim D$ is proposed according to the data. And then Eq.4 can be obtained. Therefore, a linear relationship can be identified by $f^{(-0.6)}v_a \sim D$ at different frequencies and vibrating velocities, as shown in Figure 8(b).

$$D \propto f^{-0.6}v_a \tag{4}$$

Therefore, the linear regression fitting can be carried out, as shown in Eq. 5, with the adjusted R^2 of 0.99. Thus, we establish the quantitative relationship among the vortex diameter of the streaming vortex, v_a, and frequencies.

$$D = 748 f^{-0.6}v_a \tag{5}$$

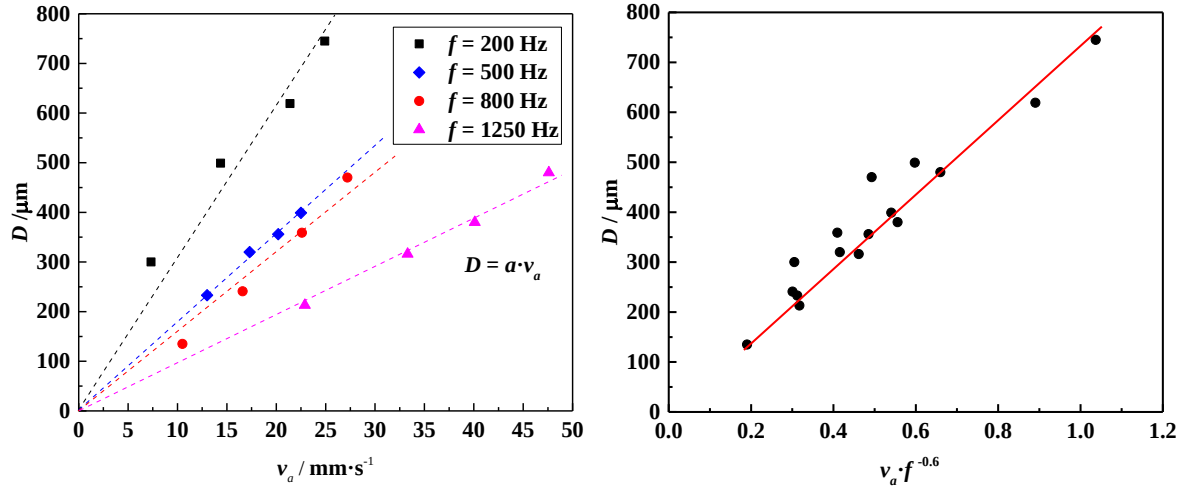

(a) (b)

Figure 8. (a) Vortex diameter D with v_a at different frequencies (b) Linear data fitting of Vortex diameter D at different forcing velocities and different frequencies

3.3. Characteristics of streaming vorticity

Figure 9 shows the vorticity contour with a different vibrating velocity of 40 mm/s ~ 65 mm/s at 2.5 kHz, based on the vector diagram by PIVlab in Figure 5. The maximum streaming vorticity in the vicinity of the sharp edge reaches 95 s^{-1} at v_a=64 mm/s, and that decreases to 20 s^{-1} when v_a goes to 40 mm/s. It shows that a stronger forcing amplitude induces a more intensive dissipation near the sharp edge, followed by a more significant vortex effect, as shown in Figure 9-d. It's reminded that the position of the vorticity center still accumulates near the sharp tips around the viscous boundary layer, although the spatial vorticity extends far to both sides of the sharp edge in the channel with the increase of velocity amplitude.

From the perspective of quantitative value and vortice pattern, the maximum vorticity on both sides of the sharp edge is not always the same, and the pair of vortices also shows deviation from each other beside the central axis of the sharp edges. This inconsistency is found to be random after repeated experiments. Except for the errors of post-processing, the fabricating process of the PDMS chips on the curvature diameters of the sharp edge will also disturb the symmetry of the vortice pairs.

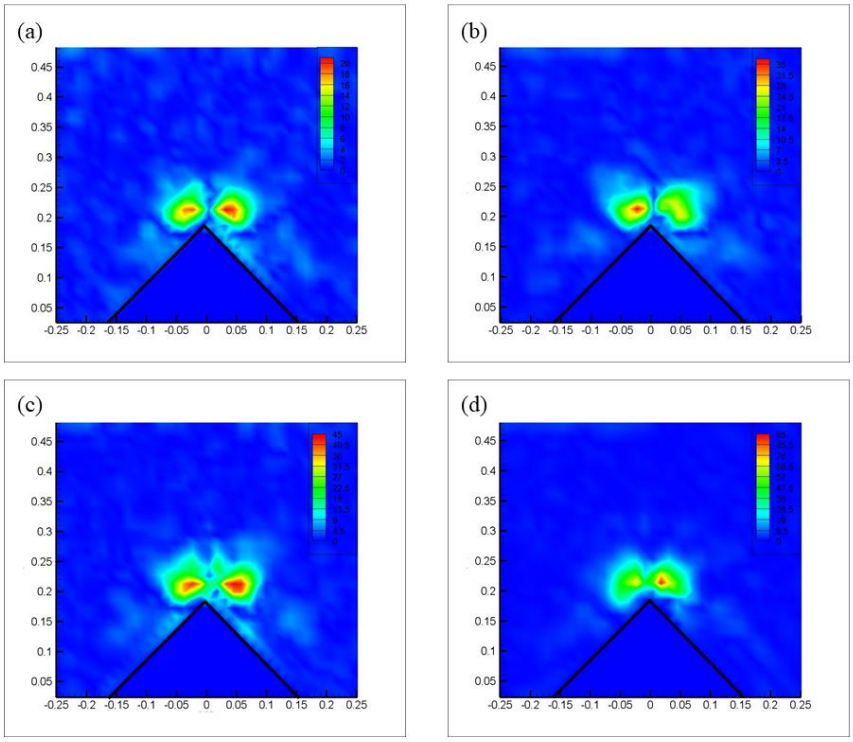

Figure 9. Vorticity of streaming flow at different forcing velocity at f = 2.5 kHz, (a) v_a =40 mm/s, (b) v_a = 46 mm/s, (c) v_a = 53 mm/s, and (d) v_a = 65 mm/s

3.4. Maximum streaming velocity influenced by the frequency and vibrating velocity

Figure 10 shows the maximum values of streaming velocity $v_{sy,\,max}$ in the normal direction of the sharp angle under the designed conditions in Table 1 with the error bar included. With the increase of the forcing amplitude, $v_{sy,\,max}$ shows a nonlinear relationship with v_a and roughly shows a quadratic relationship, namely, $v_a^2 \propto v_s$, which validates our previous study [18]. However, this relationship does not describe the frequency information, and the change rule of the maximum sound flow velocity with frequency needs further research.

In order to describe the intensity of the streaming flow induced by the sharp edge, Eq. 6 is put forward to quantify this feature by extracting the related quadratic coefficient θ after the data fitting according to Figure 10.

$$\theta = \Delta v_{sy,\max} / \Delta(v_a^2) \tag{6}$$

Where $v_{sy,\,max}$ is the maximum streaming flow velocity along the normal direction of the sharp edge. As shown in Figure 11, the streaming intensity is the same as the characteristic number $2r_c/\delta$. To describe the influence of the frequency on the streaming intensity. It can be seen that the characteristic number θ decreased with $2r_c/\delta$, which is determined by the frequency since $\delta = \sqrt{2\upsilon/\omega}$, where ω represents the angular frequency. It implies that the conversion efficiency of the first-order-flow energy to the secondary-order-flow energy at high frequency is limited. When the frequency increases from 200 Hz to 2500 Hz, the streaming intensity decreases by 34.8% from 0.00066 s/mm to 0.00043 s/mm.

In order to further quantify the relationship between $v_{sy,max}$ and v_a at different frequencies and vibrating velocity, the relationship between sharp edge acoustic streaming velocity and operating parameters obtained by Ovchinnikov et al. [25] is introduced as shown in Eq. 7.

$$v_s(r) = \frac{v_a^2}{\upsilon}\frac{\delta^{2n-1}}{h^{2n-2}} H_\alpha(\frac{r}{\delta}) \tag{7}$$

where R, h, and H_α represent the radius in the cylindrical coordinate, the height of the sharp edge, and the dimensionless coefficient of the radial velocity profile. n is the coefficient related to structural features, as $n = \pi/(2\pi - \alpha)$ with α radians of the sharp edge.

Eq. 7 can be always satisfied when $r_c < \delta$, where r_c is nearly 9.25 μm in this study and smaller than the thickness of the boundary layer. According to the previous study[18], $v_{sy,max}$ and v_a have a quadratic correlation.

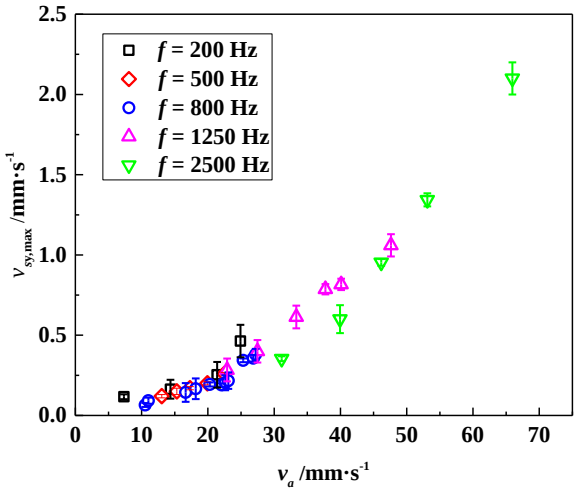

Figure 10. Maximum streaming velocity $v_{sy,max}$ with v_a at different frequencies

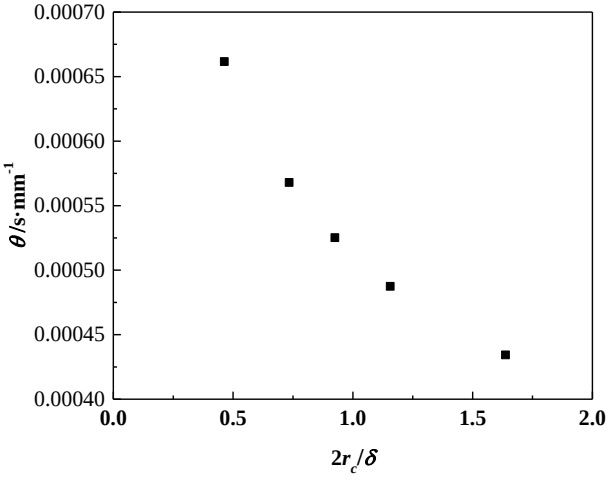

Figure 11. Streaming intensity with $2r_c/\delta$ (r_c is constant and δ changes with the frequency)

In order to describe the relationship further, α is replaced by $\pi/2$ and δ by ν and f in Eq. 7, after which Eq. 8 can be obtained. Therefore, a linear relationship can be identified by $f^{-1/6}v_a^2 \propto v_{sy,max}$ at different frequencies and forcing amplitudes, as shown in Figure 12.

$$v_s \propto f^{-1/6}v_a^2 \tag{8}$$

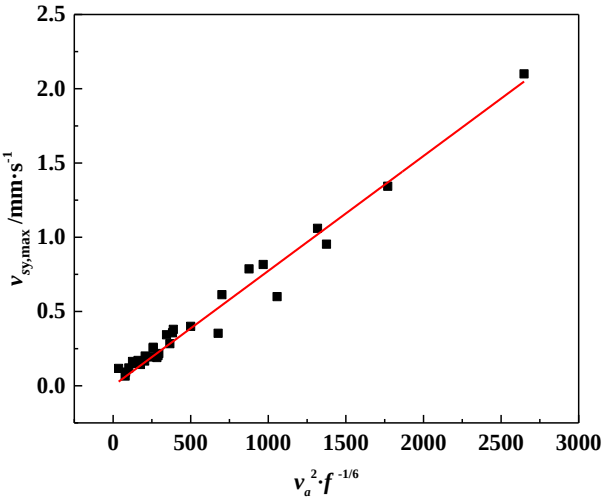

Figure 12. Linear data fitting of $f^{-1/6}v_a^2$ □ $v_{sy,max}$ at different frequencies and forcing amplitudes

Therefore, the linear regression fitting can be carried out, as shown in Eq. 9, with the adjusted R^2 of 0.99. Thus, we establish the quantitative relationship between sharp edge acoustic streaming velocity and operating parameters, which well predicts the maximum streaming velocity in the vicinity of the sharp edge, especially under high-frequency conditions.

$$v_{sy,\max} = 0.00077 f^{-1/6} v_a^2 \tag{9}$$

4. Conclusion

In this study, the effects of frequencies and velocity amplitudes on sharp-edge acoustic streaming are studied experimentally. The curvature angle and the curvature diameter are 90◦ and 18.5 ± 3.6 μm respectively, with an operating frequency of 200 Hz ~ 2500 Hz and vibrating velocity of 7.0 ~ 66 mm/s. The main conclusions are as follows:

(1) We re-validate that the streaming velocity increases with the vibrating velocity, and the profile of streaming velocity along the normal direction of the sharp edge will reach its maximum near the outer side of the boundary layer at α = 90◦, firstly raised by Zhang et al.[18], which still occurs at different frequencies. Besides, a large acoustic streaming vortex is generated on both sides of the sharp edge, which increases with the vibrating velocity. However, the vortices domain will be squeezed and deformed by the opposite wall when the enhanced streaming jet is too strong.

(2) The size of the streaming flow is quantified by introducing the vortex diameter to describe the influenced domain in the vicinity of the sharp edge. We find that the vortex diameter of vortices increases nearly linearly with the vibrating velocity. During the data fitting, we find that the higher the frequency is, the better the linear relationship behaviors.

(3) The parametric influences of frequency and vibrating velocity on streaming velocity are quantified as well with the adjusted coefficient of the linear regression R^2 approaching 0.99 by $f^{-1/6}v_a^2$ □ $v_{sy,max}$.

Nomenclature

A	Forcing amplitude[mm]

a	Linear fitting coefficient[10^{-3} s]
D	Spacial diameter of streaming vortex[μm]
f	Forcing frequency[Hz]
H_α	The dimensionless coefficient of the radial velocity profile[-]
h	Height of the sharp edge[μm]
n	n-th acoustic cycle[-]
p	Depth of channel[μm]
r_c	Tip radius of curvature[μm]
T	Period[s]
t	Time[s]
$\boldsymbol{v_a}$	Forcing vibration velocity[$m \cdot s^{-1}$]
v_a	The amplitude of vibration velocity[$mm \cdot s^{-1}$]
v_s	Streaming velocity[$mm \cdot s^{-1}$]
v_{sy}	Streaming velocity in y-oriented[$mm \cdot s^{-1}$]
$v_{sy,\ max}$	Maximum streaming velocity in y-oriented[$mm \cdot s^{-1}$]
w	Width of channed[μm]

Greek symbols

α	Tip angle of sharp edge[rad]
δ	Viscous boundary layer (VBL) thickness[μm]
μ	Dynamic viscosity[Pa·s]
v	Kinematic viscosity[$m^2 \cdot s^{-1}$]
θ	The related quadratic coefficient[$s \cdot mm^{-1}$]
ρ	Liquid density[$kg \cdot m^{-3}$]
ω	Angular frequency[$rad \cdot s^{-1}$]

Acknowledgments

This project is financially supported by the National Key R & D Program of China (2022YFC2406600), the National Key Research and Development Program of China (Grant No. 2022YFE0210200), and the Program for Innovation Team of Shaanxi Province (2021TD- 23).

References

[1] Michael, F. XVII., On a peculiar class of acoustical figures and certain forms assumed by groups of particles upon vibrating elastic surfaces, *Philos T R Soc B.*, *121* (1831), pp. 299–340.

[2] Morris, P. J., Boluriaan, S., Acoustic streaming: From Rayleigh to today, *Int J Aeroacoust*, *2* (2003), pp. 255–292.

[3] Lighthill, S. J., Acoustic streaming, *J Sound Vib*, *61* (1978), 3, pp. 391–418.

[4] Eckart, C., Vortices and streams caused by sound waves, *Physical Review*, *73* (1948), pp. 68–76.

[5] Rayleigh, L., On the circulation of air observed in Kundt's tubes and on some allied acoustical

problems, *Philos T R Soc B.*, *175* (1884), pp. 1–21.

[6] Wiklund, M., *et al.*, Acoustofluidics 14: Applications of acoustic streaming in microfluidic devices, *Lab Chip.*, *12* (2012), 14, pp. 2438-2451.

[7] Zhang, C. Y., *et al.*, Acoustic streaming near a sharp structure and its mixing performance characterization, *Microfluid Nanofluid.*, *23* (2019), pp. 104.

[8] Legay, M., *et al.*, Improvement of heat transfer by means of ultrasound: Application to a double-tube heat exchanger, *Ultrason Sonochem.*, *19* (2012), 6, pp.1194–1200.

[9] Byoung-Gook, L., *et al.*, Acoustic streaming induced by ultrasonic flexural vibrations and associated enhancement of convective heat transfer, *J Acoust Soc Am.*, *111* (2002), 2, pp.875–883.

[10] Huang, P. H., *et al.*, An acoustofluidic micromixer based on oscillating sidewall sharp edges, *Lab Chip.*, *13* (2013), pp. 3847–3852.

[11] Huang, P. H., *et al.*, A reliable and programmable acoustofluidic pump powered by oscillating sharp-edge structures, *Lab Chip.*, *14* (2014), 22, pp. 4319-4323.

[12] Nama, N., *et al.*, Investigation of acoustic streaming patterns around oscillating sharp edges, *Lab Chip.*, *14* (2014), 15, pp. 2824-2836.

[13] Ovchinnikov, M., *et al.*, Acoustic streaming of a sharp edge, *J Acoust Soc Am.*, *136* (2014):1, pp. 22–29.

[14] Costalonga, M., *et al.*, Low-frequency vibration induced streaming in a Hele-Shaw cell, *Phys Fluids.*, 27 (2015), 1, pp. 013101.

[15] Zhang, C. Y., *et al.*, Mixing intensification using sound-driven micromixer with sharp edges, *Chem Eng J.*, *410* (2021), pp. 128252.

[16] Nama, N., *et al.*, Investigation of micromixing by acoustically oscillated sharp edges, *Biomicrofluidics.*, *10* (2016), 2, pp. 024124.

[17] Lei, J. J., *et al.*, Effects of micron-scale surface profiles on acoustic streaming, *Microfluid Nanofluid.*, *22* (2018), pp. 140.

[18] Zhang, C. Y., *et al.*, Unveiling of the mechanisms of acoustic streaming induced by sharp edges, *Physical Review E.*, *102* (2020), pp. 043110.

[19] Zhong, G. Y., *et al.*, Vibration induced streaming flow near a sharp edge: Flow structure and instabilities in a large span of forcing amplitude, *Physical Review E.*, *107* (2023), 2, pp. 025102.

[20] Zhang, C. Y., *et al.*, Acoustic streaming generated by sharp edges: the coupled influences of liquid viscosity and acoustic frequency, *Micromachines Basel.*, *11* (2020), 6, pp. 607.

[21] Oberti, S., *et al.*, Microfluidic mixing under low-frequency vibration, *Lab Chip.*, *9* (2009), pp. 1435– 1438.

[22] Graham, J. M. R., The forces on sharp-edged cylinders in oscillatory flow at low keule- gan–carpenter numbers, *J Fluid Mech.*, *97* (1980), 2, pp. 331–346.

[23] Tao, L. B., Thiagarajan, K., Low kc flow regimes of oscillating sharp edges i. vortex shedding observation, *Appl Ocean Res.*, *25* (2003), 1, pp. 21–35.

[24] Dual, J., Möller, D., Acoustofluidics 4: Piezoelectricity and application in the excitation of acoustic fields for ultrasonic particle manipulation, *Lab Chip*., *12* (2012), 3, pp. 506—514.

[25] Ovchinnikov, M. Y., *et al.*, Acoustic streaming of a sharp edge, *J Acoust Soc Am*., *136* (2014), 1, pp. 22–29.

Received: 15.07.2023.
Revised: 04.09.2023.
Accepted: 10.10.2023.